Any immersion remote refocus (AIRR) microscopy

This project is maintained by amsikking in the York lab, and was funded by Calico Life Sciences LLC

Research article

Note that this is a limited PDF or print version; animated and interactive figures are disabled. For the full version of this article, please visit one of the following links: https://amsikking.github.io/any_immersion_remote_refocus_microscopy

Any immersion remote refocus (AIRR) microscopy

Alfred Millett-Sikking[1*]

[1]*Calico Life Sciences LLC, South San Francisco, CA 94080, USA*

[*] *Institutional email: amsikking+AIRR@calicolabs.com ; Permanent email: amsikking+AIRR@gmail.com*

Group website: andrewgyork.github.io

Abstract

We present a new approach to aberration-free 3D imaging with remote refocus optics, where an objective of any immersion can be combined with a sample of any refractive index (RI). Normally, we optimize standard focus and remote refocus (RR) optics for the same sample RI, yielding the maximum diffraction limited depth for both focus methods. However, we make the argument that which RI we optimize for in standard focus and RR is an independent choice, which counterintuitively leads to some intriguing design options. We discover a deeper immersion-free microscopy regime by using an air objective with a RR optimized for liquid. For example, we can extend the range of a Nikon 40x0.95 air objective from 6μm to 151μm in water (standard focus vs RR). Avoiding liquid immersion can be very convenient for users and great for automated microscopy, like high-throughput screening. We also find deeper maximum numerical aperture (NA) microscopy for live biology by

using a high NA oil objective with RR optics set for watery samples. For example, we can extend the range of a Nikon 40x1.30 oil objective from 8µm to 65µm in water, and enjoy a field of view and NA that exceeds the equivalent water immersion objective. Furthermore, we can combine these new imaging regimes into a single extended range multi-immersion system, with immersion-free, maximum depth and maximum NA modalities. Moreover, we present a dynamic zoom lens to enable fast RR tuning in the refractive index range 1.33-1.51, which maximizes performance for a diverse range of biological samples. The design ideas we explore here are readily applied to systems with existing RR optics, like single-objective light-sheet (SOLS) microscopes.

Intended audience

Microscope users, builders and developers.

Peer review status

First published _blank_ (This article is not yet peer-reviewed)

Cite as: _blank_

Introduction

Choosing an objective lens is one of the most important considerations when using a visible light microscope. For example, an objective's numerical aperture (NA) and field of view (FOV) will determine the maximum available resolution and object size in the image. When we image 3D semi-transparent samples at high NA, it is necessary to adjust the focal plane to access the volumetric information. For example, we often move the objective towards the object to get a series of 2D images at different depths, a method we refer to as "standard focus". The maximum imaging depth of a typical widefield microscope is therefore ultimately limited by the working distance (WD) of the objective.

The positive working distance we need for standard focusing contains the 'final elements' in the objective lens design, where the shape and refractive index (RI) matter. Fortunately, the shape is fixed by the image plane and the final solid surface of the objective (usually a glass lens). However, the RI of this space can vary, i.e. the *immersion* medium (and sometimes a coverslip). When we use standard focus to image deeper, 'slabs' of intended immersion (like air, water or oil) are effectively exchanged for slabs of sample. If the sample RI matches the immersion RI, then this is a null operation and the objective will image as designed (Figure 1, 1/3). However, if there is a refractive index *mismatch*, then the slab of sample (with unintended RI) will produce spherical aberration at finite NA, making the images blurry with enough depth (Figure 1, 2/3 and 3/3) [Pawley 2006].

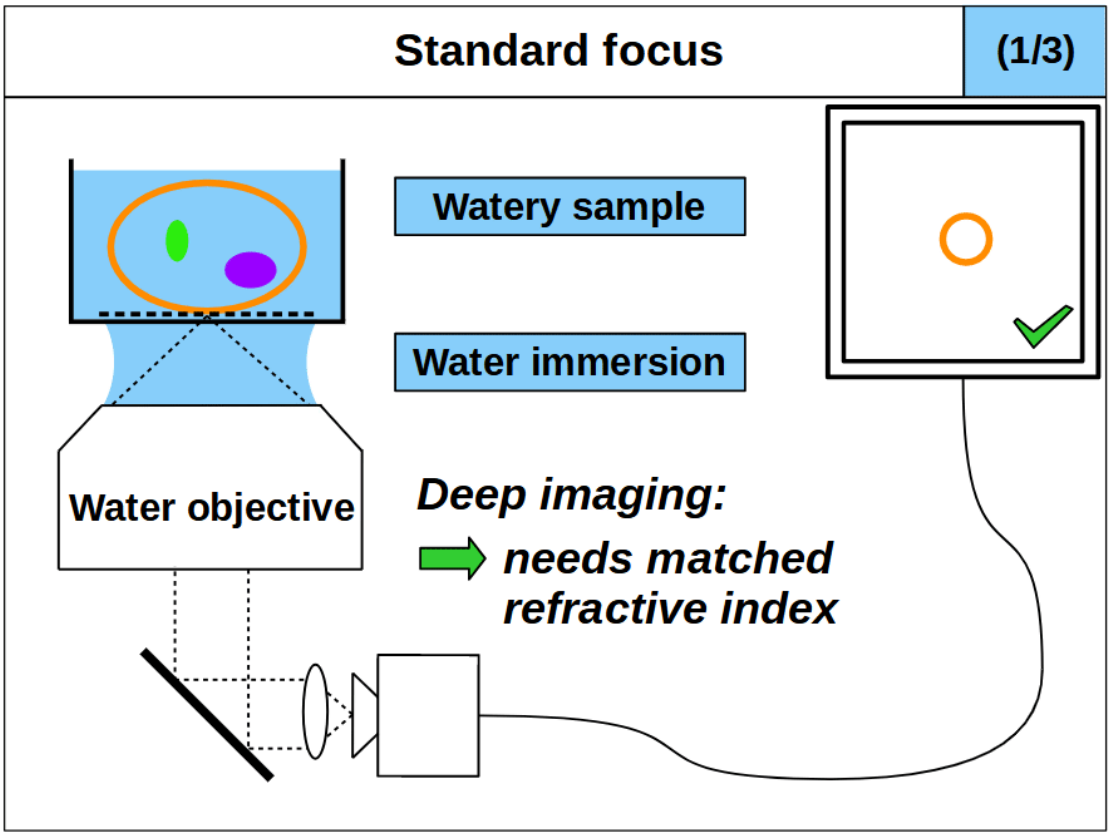

Figure 1: Standard focus into a watery sample with water, air and oil immersion. This cartoon shows a watery 3D sample (like a cell in media) being imaged at different depths by a standard widefield microscope (objective and tube lens pair). The image is formed at the camera and relayed to the toy screen, which shows image planes at different depths in the sample as the objective moves up and down. **Animation 1/3** shows a water immersion objective that is refractive index *matched* to the sample, giving good images at depth. **Animation 2/3** shows an air objective that is refractive index *mismatched* to the sample and therefore gives blurry imaging from depth induced spherical aberration. **Animation 3/3** shows an oil immersion objective that (like animation 2/3) is also refractive index *mismatched* giving blurry images with depth.

So, it follows that for aberration-free standard focusing, we must set the immersion refractive index n_i equal to the sample refractive index n_s:

$$n_i = n_s \tag{1}$$

Our need to refractive index *match* the immersion to the sample for 3D imaging is awkward. The RI of biological samples varies significantly, leaving microscope users (and lens designers) chasing around between different immersion options. Air immersion is the most convenient and is excellent for high-speed tiling, but it has the lowest NA and low depth penetration due to the large RI difference. Water immersion is usually a good RI match for live samples, but it requires regular hydration (from evaporation) and has the lowest NA of the liquid immersions. Oil immersion offers the highest NA and is insensitive to coverslip thickness but struggles with depth from the RI mismatch. A good compromise between NA and RI matching is silicone oil immersion, but this is still cumbersome in tiling applications.

Remote refocus (RR) optics [Botcherby 2007] are an important foundation in high-speed 3D imaging applications [Millett-Sikking 2018], most notably in the recent uptake of single-objective light-sheet (SOLS) microscopes [Millett-Sikking 2019, E. Sapoznik 2020, Chang 2021, Yang 2022, Chen 2022]. The main feature of an RR setup is our ability to adjust the focal plane without moving the primary objective or the sample, for example by moving one of the downstream objectives (Figure 2, 1/3). In a remote refocus we can exchange slabs of *different* refractive index between the sample and the remote volume. For example, it is common to use air immersion in the remote space with an aqueous sample. We avoid spherical aberration by setting the magnification between the sample and remote space to preserve angles:

$$M_{RR} = \frac{n_s}{n_{RR}} \tag{2}$$

where M_{RR} is the RR magnification and n_{RR} is the immersion of the remote space. **So we should always optimize the remote refocus for the refractive index of the sample, not the immersion of the objective.**

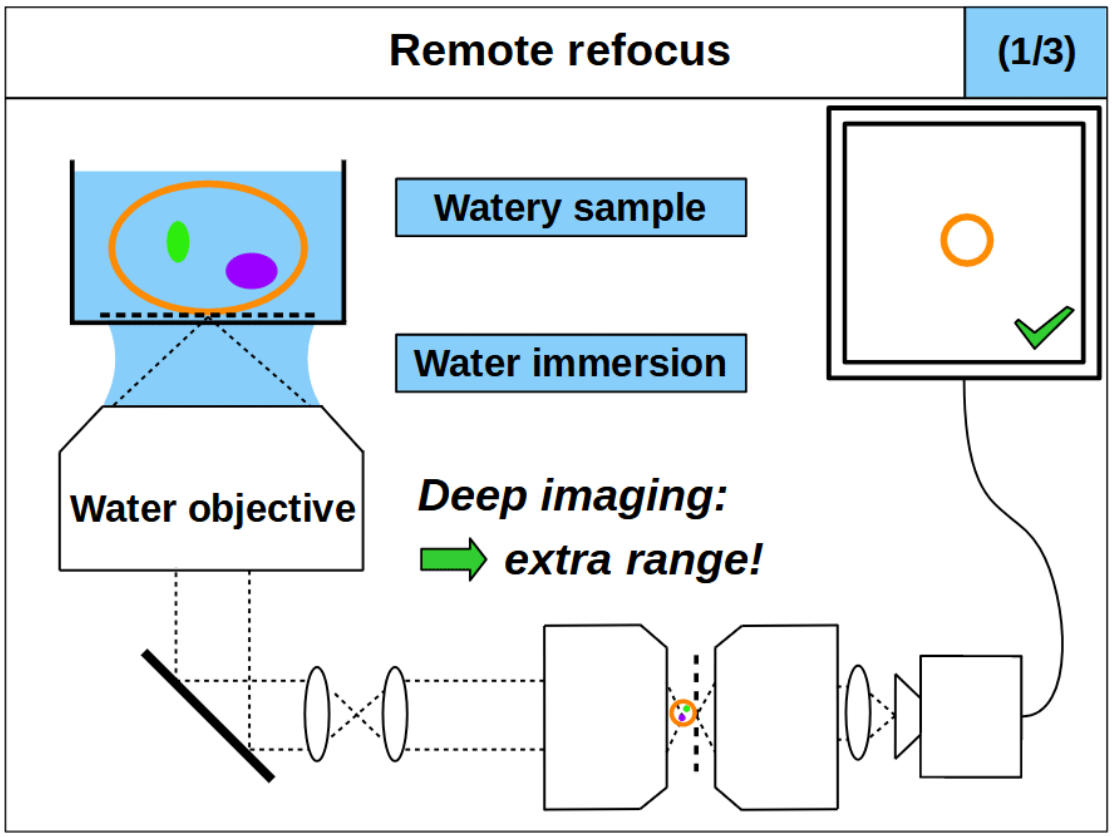

Figure 2: Remote refocus into a watery sample with water, air and oil immersion. This cartoon shows a watery 3D sample (like a cell in media) being imaged at different depths by a remote refocus microscope (a widefield + 2 additional microscopes). The optics in the first 2 microscopes (widefield + tube lens objective pair) are configured to produce an aberration-free 3D copy of the sample in the remote space, which is then re-imaged by the 3rd microscope (objective tube and lens pair). **Note: the remote refocus optics are set for a watery sample, regardless of the immersion used by the primary objective.** The final image is formed at the camera and relayed to the toy screen, which shows image planes at different depths in the sample as the objective in the 3rd microscope moves back and forth. **Animation 1/3** shows a water immersion objective that is refractive index *matched* to the sample. In this configuration the standard focus

and remote focus both have maximum range, although only the remote focus range is animated here (giving extra range). **Animation 2/3** shows an air objective that is refractive index *mismatched* to the sample, greatly reducing the range of standard focus. However, the remote refocus is still optimized for a watery sample, and so the remote range persists. **Deeper immersion-free microscopy** is available in this configuration. **Animation 3/3** shows an oil immersion objective that (like animation 2/3) is also refractive index *mismatched* (reducing the range of standard focus). However, like animation 2/3, the remote refocus is still optimized for a watery sample and the range persists. **Deeper maximum NA microscopy** is available in this configuration.

In a typical system we would match the sample and immersion RI (equation 1), and we would correct the RR magnification for the sample (equation 2), yielding maximum range for both standard focus and remote refocus. If however, the RI of the sample and immersion differ, then the range of standard focusing will reduce, but the remote refocus range persists. Conversely, if we match the sample and immersion RI, but the remote refocus is optimized for a different RI, then the RR range will reduce and the standard focus range will persist. **So which refractive index we optimize for in standard focus and remote refocus is an independent choice**.

It is counter intuitive to deviate from the 'usual' system design, where we optimize the immersion and remote refocus for the same sample RI. However, upon closer inspection there are some intriguing options:

- **Deeper immersion-free microscopy:** we can combine a high NA air objective (with very limited standard focus range in liquids) with a remote refocus optimized for liquid (Figure 2, 2/3). Avoiding liquid immersion is very convenient for users and great for automated microscopy, like time-lapse imaging or high-speed tiling.
- **Deeper maximum NA microscopy:** we can combine a high NA oil objective (with reduced standard focus range in watery samples) with a remote refocus optimized for water (Figure 2, 3/3). Oil immersion is coverslip insensitive and offers the maximum NA for live biological samples, exceeding that of high quality water immersion objectives.

We gear the rest of this article towards *how* to choose an objective lens in combination with RR optics in the context of high NA microscopy, like SOLS microscopes.

Results

To evaluate the deeper imaging potential of a remote refocus microscope (Figure 2) compared to a widefield setup (Figure 1), we take a practical approach and model how a series of commercially available objectives compare in each configuration. For the sake of simplicity, we limit our search to a collection of Nikon objectives that are compatible with SOLS microscope design (a compelling use case for RR optics). We can therefore constrain the numerical aperture, focal length and immersion medium for a given setup, although we point out that these ideas can be applied to other manufacturers, and at lower NA. We can then calculate the standard focus and remote refocus ranges as a function of the sample refractive index n_s over the biological range:

$$1.33 \leq n_s \leq 1.51 \tag{3}$$

In Figure 3 we compare the accessible imaging range of different objectives in a widefield microscope, by plotting the diffraction limited depth of standard focus as a function of the sample RI (equation a8). The interactive figure can be toggled between linear and log scales for the highest NA objectives, and those with the 'most pixels' (N_{px}). For example, in the high NA category, the 100x1.35 silicone oil objective offers the best compromise for varying sample types, with a minimum range of 10µm for any RI. However, if the samples are mostly aqueous, then the 60x1.27 water lens has a much larger range (limited by the working distance at 180µm). The 40x0.95 air objective is perhaps the worst option for depth, offering only ~6µm for any liquid sample (visible on the log scale). The 100x1.45 oil may be the least attractive option for live biology, with the inconvenience of liquid immersion and the lowest range in watery samples (forcing the 3µm lower bound). Similar trends can be seen in the most pixels category.

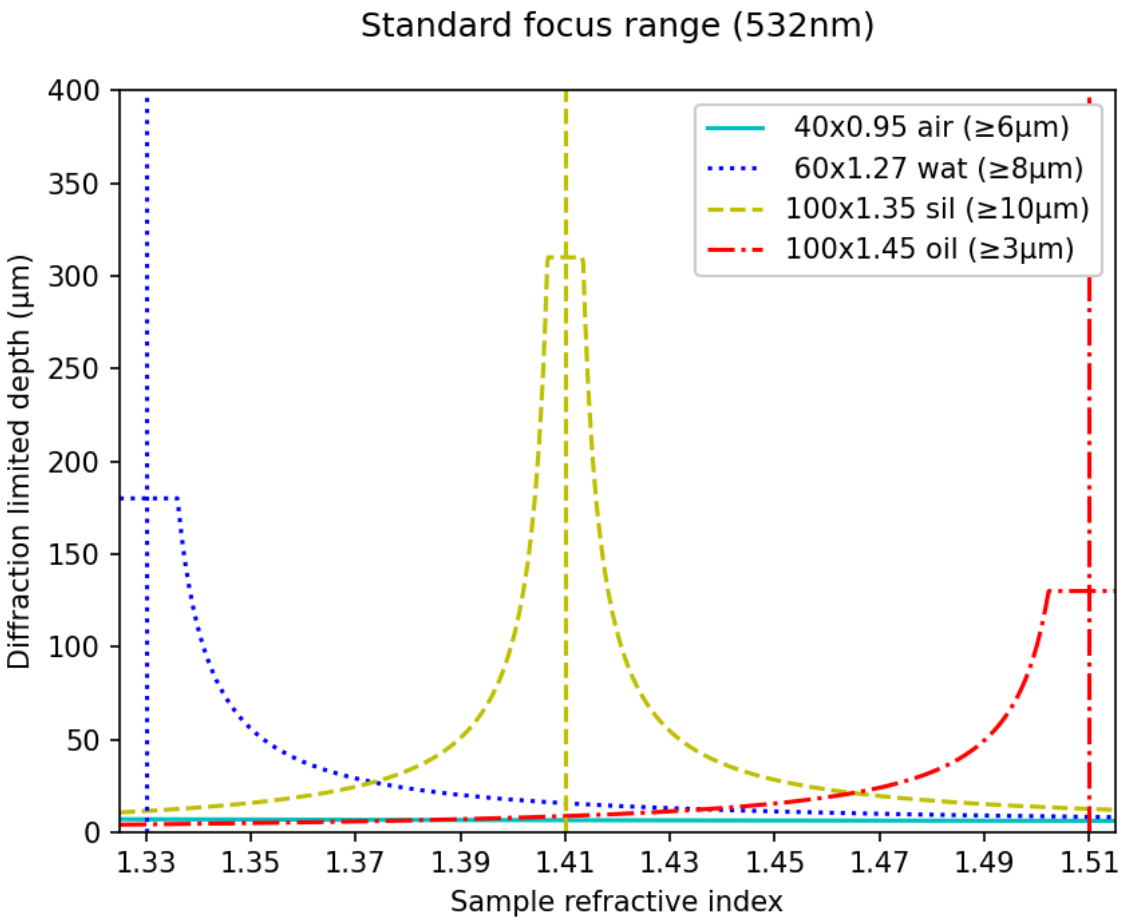

Nikon objectives: Highest NA ▾ Depth scale: linear ▾

Figure 3: the standard focus range of a widefield microscope. The diffraction limited imaging depth is plotted as a function of sample refractive index for a collection of Nikon objectives at 532nm (equation a8). The figure is interactive and can be toggled between linear and log scales for objectives with the highest NA and those with the most pixels. The curves are truncated at the working distance of each objective and vertical reference lines are added for the standard immersions (water=1.33, silicone=1.41 and oil=1.51).

In Figure 4 we present the combined range of a widefield microscope with remote refocus optics (equation a11). In this setup, the primary objectives are still limited to a particular immersion, but we can (in principle) optimize the remote refocus optics continuously across the range of the sample RI (shown here). All of the configurations

now benefit from the extra range provided by the RR optics. In particular, in the high NA category the lower bound on the 100x1.45 oil lens has now jumped from 3µm to 35µm, converting it into an attractive option for many applications. In practice, this delivers deeper imaging at **maximum NA** for any sample RI under 1.45. Most apparent in the high NA category is the large increase in depth now available to the 40x0.95 air objective, offering deeper **immersion-free** imaging up to 151µm!

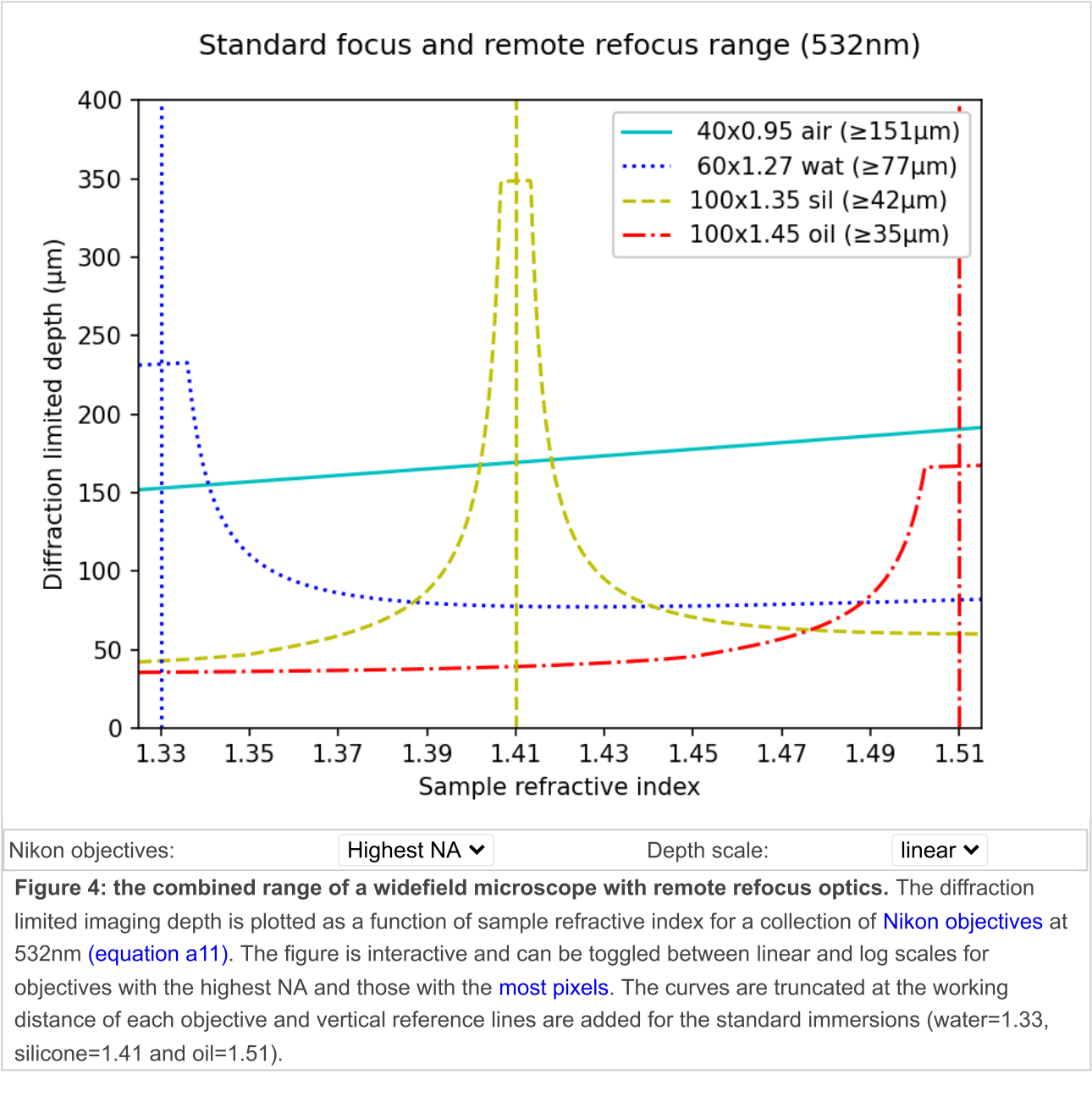

Figure 4: the combined range of a widefield microscope with remote refocus optics. The diffraction limited imaging depth is plotted as a function of sample refractive index for a collection of Nikon objectives at 532nm (equation a11). The figure is interactive and can be toggled between linear and log scales for objectives with the highest NA and those with the most pixels. The curves are truncated at the working distance of each objective and vertical reference lines are added for the standard immersions (water=1.33, silicone=1.41 and oil=1.51).

In the introduction, we discuss how the RR magnification should be set according to equation 2, and that we should always optimize for the sample (not the immersion). Previously, we used static optical configurations to set the RR magnification for a particular sample refractive index [Millett-Sikking 2019], with the hope that the sample RI would not deviate much from the immersion of the primary objective. Here we present a dynamic zoom lens to enable fast RR tuning in the refractive index range 1.33-1.51, which maximizes performance for a diverse range of biological samples (Figure 5). Our example uses inexpensive stock parts, maintains constant

track length and telecentricity, and is diffraction limited across the visible spectrum and standard sCMOS field of view (see appendix for details).

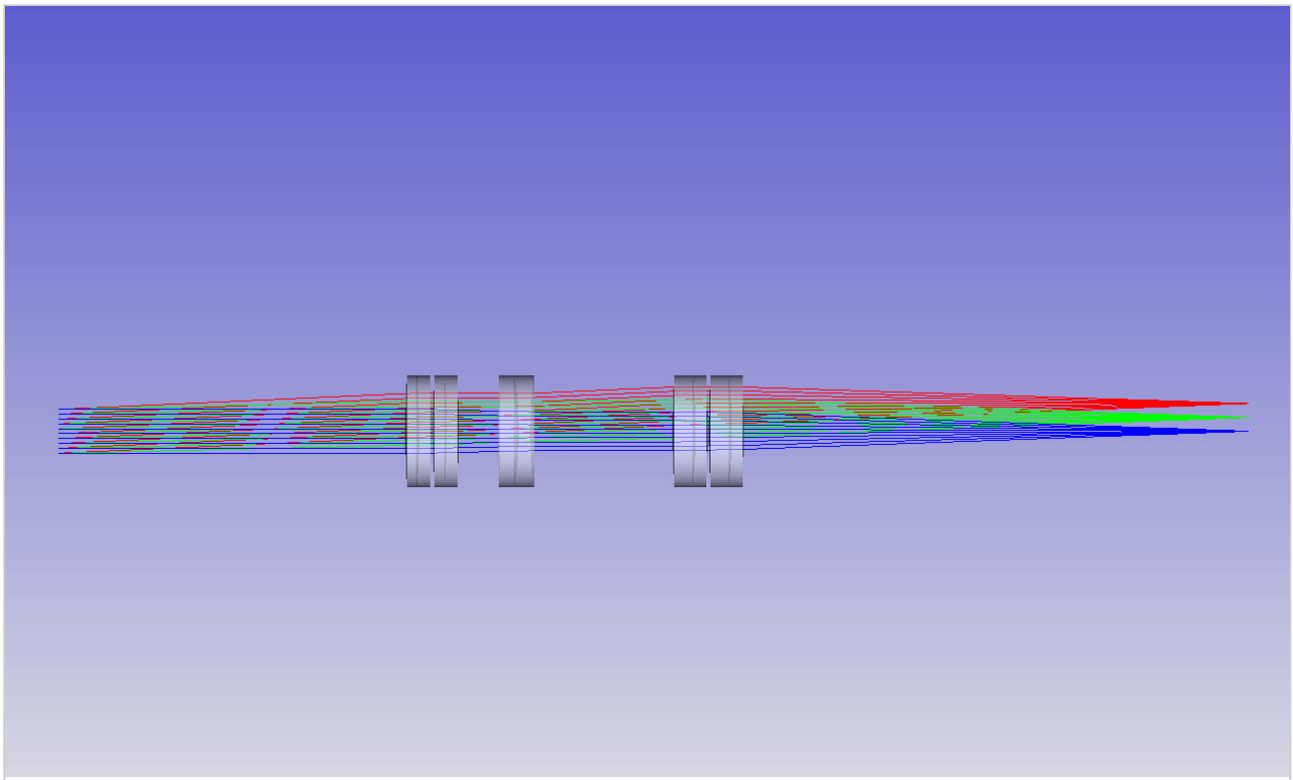

Figure 5: Dynamic zoom tube lens. This animation shows an example of a zoom lens that can replace a static tube lens in a remote refocus microscope. In this version the focal length varies continuously as the elements are moved, allowing the magnification of the RR to be tuned accross the biological refractive index range 1.33-1.51. The lens uses inexpensive stock parts, maintains constant track length and telecentricity, and is diffraction limited accross the visible spectrum and standard sCMOS field of view (see appendix for details).

Data

To demonstrate the power of this approach we built a prototype large field of view SOLS microscope with (static) remote refocus optics tuned for water (see here for current instrument details). We used this platform to directly **compare a Nikon 40x1.15 water objective against a Nikon 40x0.95 air objective**, both imaging deep into a watery gel filled with fluorescent beads. We use the water objective as the 'benchmark' for a typical optical configuration, where the immersion and sample have the same RI, and so the volumetric point spread function (PSF) is insensitive to standard focus (Figure 6). The main benefits of this modality are increased NA and total focus range (i.e. standard plus remote refocus), in exchange for the inconvenience of the immersion.

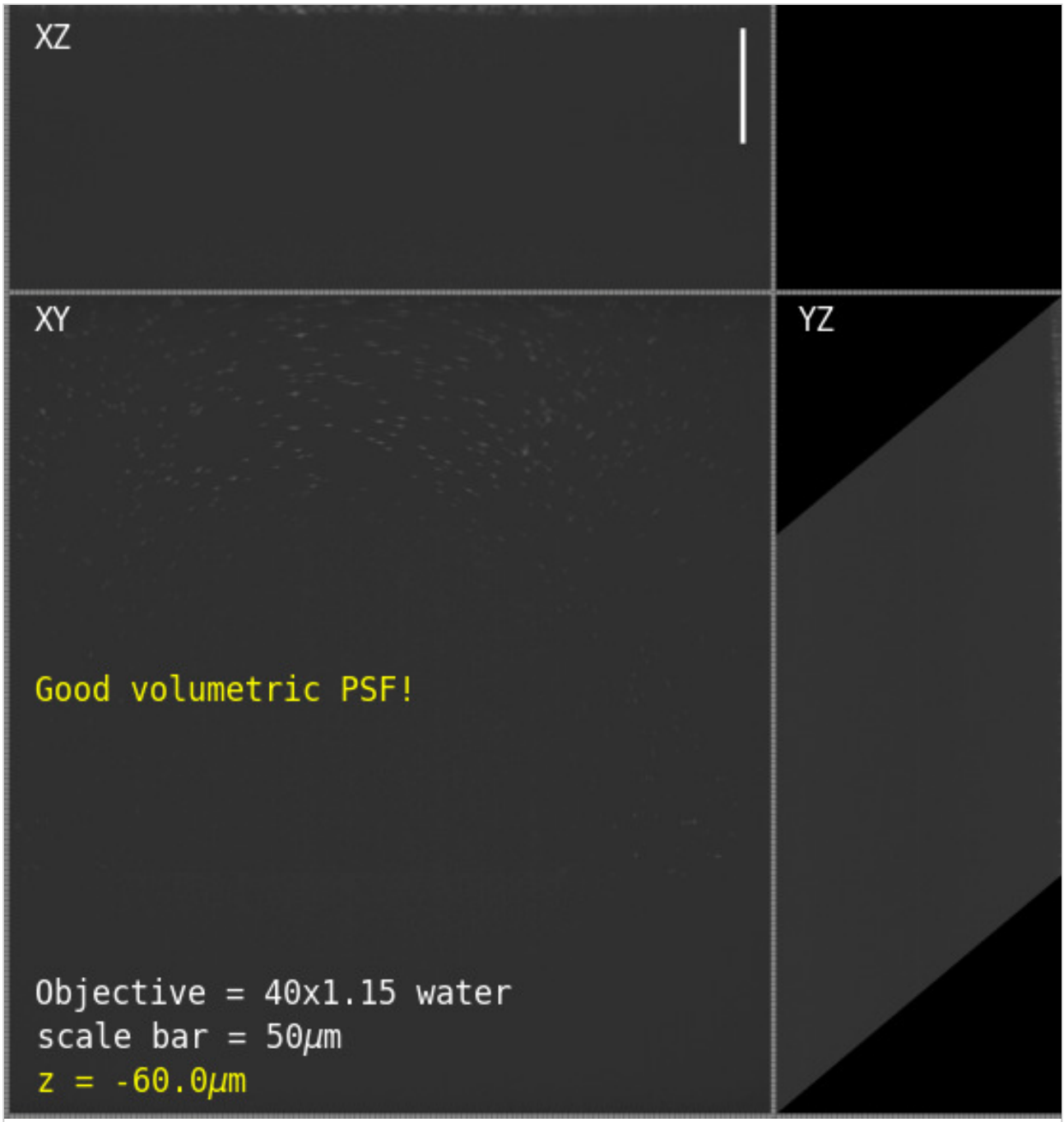

Figure 6: PSF vs standard focus for a 40x1.15 water objective. This animation shows the volumetric point spread function of a Nikon 40x1.15 water immersion objective as a function of standard focus (z). The flourescent beads were prepared in a watery gel according to this protocol. Since the sample RI *matches* the water immersion the PSF is insensitive to standard focus, allowing an increased range of focus (standard + remote) when using the microscope in this modality. **Note:** each frame of the animation shows the max projections of the entire volume (~330x355x125)μm^3 in traditional XY, XZ and YZ coordinates.

We can now *swap* the water objective for the air objective and (perhaps counterintuitively!) get good volumetric PSF *deep* into the watery gel. This modality has the benefit of being immersion-free, with the drawback of reduced NA and standard focus range (about ~6μm in agreement with Figure 3).

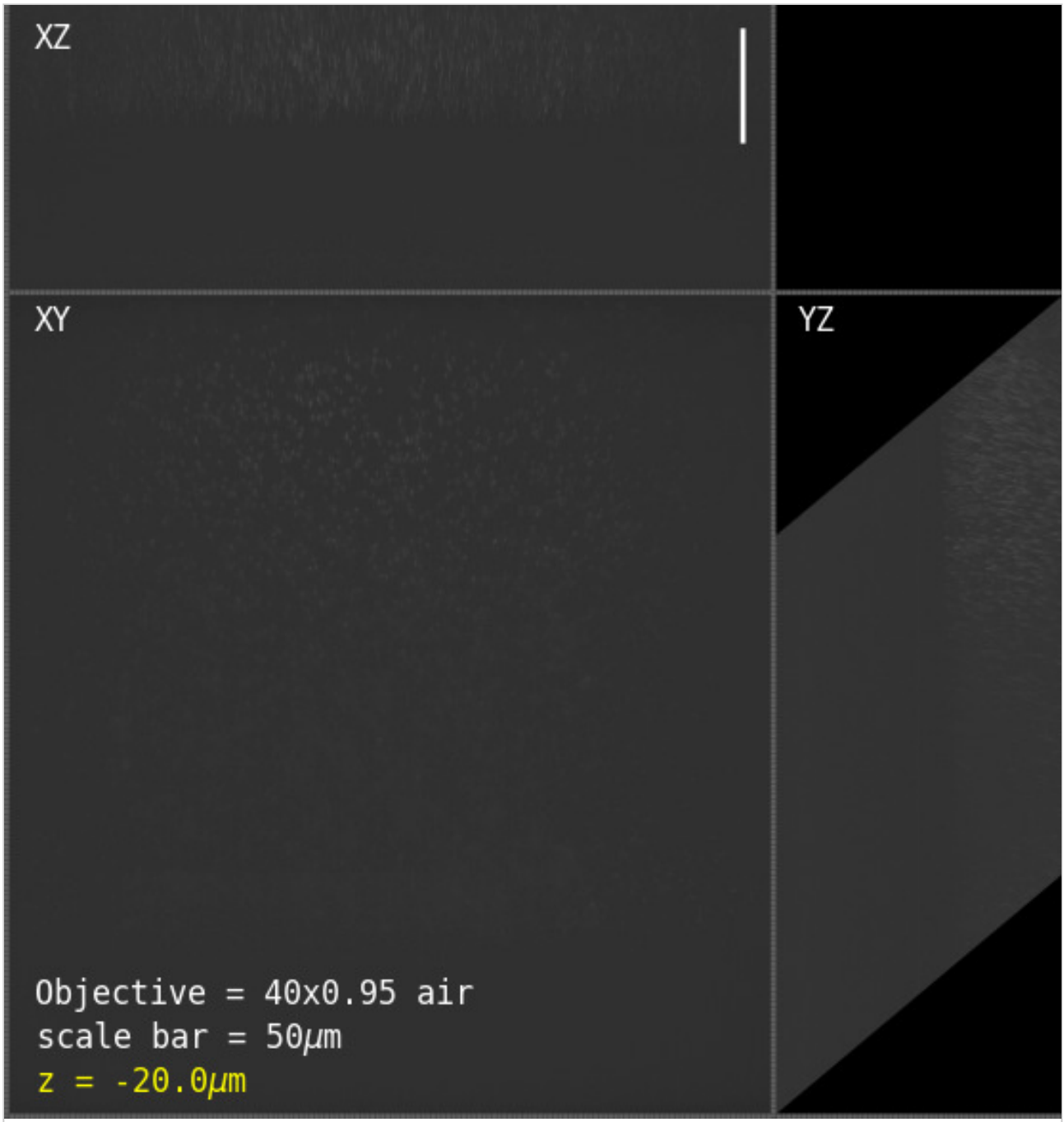

Figure 7: PSF vs standard focus for a 40x0.95 air objective. This animation shows the volumetric point spread function of a Nikon 40x0.95 air objective as a function of standard focus. The flourescent beads were prepared in a watery gel according to this protocol. Since the sample RI strongly *mismatches* the air immersion the PSF is highly sensitive to standard focus. However, as predicted by the results section, there is a ~6μm range over which the remote refocus volume is good, allowing deeper immersion-free imaging when using the microscope in this modality (i.e. for convenience or high speed tiling etc). **Note:** each frame of the animation shows the max projections of the entire volume (~330x355x125)μm^3 in traditional XY, XZ and YZ coordinates.

If we 'park' the standard focus in a good place for both the water and air objectives (i.e. at 'zero' depth where the focal plane is just above the coverslip) then we can compare the volumetric PSF in both configurations (~330x195x65)μm^3. For the **water objective PSF** we found full width half max (FWHM) values in the range **(425-582)nm radially and (1.38±0.11)μm axially** (2577 beads used for statistics). For the **air objective PSF**

we found FWHM values in the range **(422-550)nm radially and (2.08±0.07)µm axially** (2716 beads). As expected the water objective has notably improved axial PSF due to the higher NA. The higher NA should also show in a reduced radial PSF but the current instrument prototype was originally optimized for the air objective so there is some vignetting at objective 2 and the pixel size (~220nm) is too large (addressed here with an improved configuration). Overall these PSF results are in line with similar microscopes like DaXi which gave (380-480)nm radial and (1.86±0.17)µm axial [Yang 2022] or tiling OPM with (390-430)nm radial and (1.22±0.13)µm axial [Chen 2022].

Discussion

The question of *which* objective or remote refocus optics are optimal for a given microscope (or application) may be confusing to the novice or seem dull to the seasoned microscopist. However, we clearly show in the results section that whether considering a widefield or RR setup, the accessible focal range depends strongly on these choices. To highlight some interesting options, we target the discussion towards *watery samples* that are most relevant to 3D time-lapse imaging, like living cells and organisms.

In a widefield microscope for any sample RI under ~1.36, we can clearly see that the 60x1.27 water objective has the highest diffraction limited depth (Figure 3). In this regime the other objectives (air, silicone and oil) should only be considered for very shallow 3D samples (< 10µm) or speciality situations where the lack of immersion or marginal increase in NA are required (like high-speed 2D tiling or TIRF). With a 333µm field of view, a theoretical resolving power of ~250nm and ~2600 pixels, the 60x water objective is a good match for current sCMOS cameras and a compelling option (specifications from table). Although water objectives are sensitive to coverslip tilt, thickness and require regular hydration, the 60x1.27 clearly offers the best 3D imaging performance in the high NA category.

In a remote refocus microscope (like a SOLS system), we present a new series of interesting options that significantly outcompete widefield in terms of volumetric range and NA (Figure 4). For example, we can combine an RR optimized for water with multiple objectives, like a 40x1.15 water objective (MRD77410) for **maximum depth** (600µm WD), a 40x0.95 air objective for **immersion-free** speed and convenience, and a 40x1.30 oil objective for **maximum NA**. Because these lenses have the same focal length they are *interchangeable* on the same system, and at 40x magnification, they offer larger fields of view (500µm) and pixel counts (> 2927) than the 60x1.27 water objective (the leading widefield option). As an additional benefit, we also note that a sample optimized RR avoids the axial 'stretching' (when $n_i > n_s$) and 'squashing' (when $n_i < n_s$) distortions from using standard focus with mismatched immersion [Diel 2020].

We assert that remote refocus optics should always be configured for the sample refractive index, and not the objective immersion. We acknowledge that for the same or similar samples this may be achieved with static optical configurations. However, we present a dynamic zoom lens to quickly tune the RR optics for the biological refractive index range 1.33-1.51, which maximizes system performance. This has the *additional benefit* of keeping excitation light aligned with the remote volume at different sample RI (as is needed for example in a

SOLS microscope). **We propose that a dynamic magnification compensator is the correct way to build a remote refocus microscope when imaging samples of varied refractive index.**

We find the **immersion-free** configurations particularly attractive for high throughput screening applications [Maioli 2016], where the benefit of high-speed tiling can greatly outweigh the slightly lower NA of an of air objective compared to liquid immersion options. In this regime, the increase in depth of a remote refocus microscope over a widefield is substantial, for example 151µm vs 6µm for the 40x0.95 air objective. We also find the thermal isolation from the 'air gap' appealing, avoiding the need to heat the objective for incubated samples.

We see the coverslip insensitive oil immersion options with **maximum NA** as a great option for 3D super resolution [Zanacchi 2011] and low light experiments [Betzig 2006] that benefit from the highest angular collection at the primary objective. For example, the 40x1.30 oil objective from the 'most pixels' category can now be considered near maximum NA for water samples up to a diffraction limited depth of 65µm, making it an impressive option for many applications.

Given the 'mix and match' nature of the design space and the strong dependency on sample RI, we encourage builders to absorb the ideas presented here, run their own calculations, and then build the best system for their application.

Acknowledgements

This work was funded and supported by Calico Life Sciences LLC, and we would like to acknowledge the fantastic research environment that has been created here by the senior staff. We have enjoyed a spectacular level of freedom and support that has made this work possible.

In particular we acknowledge Andrew G. York for the uniquely innovative environment he has championed at Calico, and his ongoing scientific mentorship and support.

Appendix

Additional details can be found in the appendix.

References

1. [Pawley 2006] Handbook of Biological Confocal Microscopy, third edition; J. Pawley; Springer US, ISBN 978-0-387-25921-5, eBook ISBN 978-0-387-45524-2, (2006) https://doi.org/10.1007/978-0-387-45524-2
2. [Botcherby 2007] An optical technique for remote focusing in microscopy; E.J. Botcherby, R. Juškaitis, M.J. Booth and T. Wilson; Optics Communications, vol 281(4), p880-887, (2007) https://doi.org/10.1016/j.optcom.2007.10.007

3. [Millett-Sikking 2018] Remote refocus enables class-leading spatiotemporal resolution in 4D optical microscopy; A. Millett-Sikking, N.H. Thayer, A. Bohnert and A.G. York; (2018) https://doi.org/10.5281/zenodo.1146083
4. [Millett-Sikking 2019] High NA single-objective light-sheet; A. Millett-Sikking, K.M. Dean, R. Fiolka, A. Fardad, L. Whitehead and A.G. York; (2019) https://doi.org/10.5281/zenodo.3244420
5. [E. Sapoznik 2020] A versatile oblique plane microscope for large-scale and high-resolution imaging of subcellular dynamics; E. Sapoznik, B. Chang, J. Huh, R.J. Ju, E.V. Azarova, T. Pohlkamp, E.S. Welf, D. Broadbent, A.F. Carisey, S.J. Stehbens, K. Lee, A. Marín, A.B. Hanker, J.C. Schmidt, C.L. Arteaga, B. Yang, Y. Kobayashi, P.R. Tata, R. Kruithoff, K. Doubrovinski, D.P. Shepherd, A. Millett-Sikking, A.G. York, K.M. Dean and R.P. Fiolka; (2020) https://doi.org/10.7554/eLife.57681
6. [Chang 2021] Real-time multi-angle projection imaging of biological dynamics; B. Chang, J.D. Manton, E. Sapoznik, T. Pohlkamp, T.S. Terrones, E.S. Welf, V.S. Murali, P. Roudot, K. Hake, L. Whitehead, A.G. York, K.M. Dean and R.P. Fiolka; (2021) https://doi.org/10.1038/s41592-021-01175-7
7. [Yang 2022] DaXi—high-resolution, large imaging volume and multi-view single-objective light-sheet microscopy; B. Yang, M. Lange, A. Millett-Sikking, X. Zhao, J. Bragantini, S. VijayKumar, M. Kamb, R. Gómez-Sjöberg, A.C. Solak, W. Wang, H. Kobayashi, M.N. McCarroll, L.W. Whitehead, R.P. Fiolka, T.B. Kornberg, A.G. York and L.A. Royer; (2022) https://doi.org/10.1038/s41592-022-01417-2
8. [Chen 2022] Increasing the Field-of-View in Oblique Plane Microscopy via optical tiling; B. Chen, B. Chang, F. Zhou, S. Daetwyler, E. Sapoznik, G.M. Gihana, L.P. Castro, M.C. Sorrell, K.M. Dean, A. Millett-Sikking, A.G. York and R.P. Fiolka; (2022) https://doi.org/10.1364/BOE.467969
9. [SOLS microscopes] High NA single-objective light-sheet; A. Millett-Sikking, K.M. Dean, R. Fiolka, A. Fardad, L. Whitehead and A.G. York; (2019) https://doi.org/10.5281/zenodo.3244420
10. [like a SOLS system] High NA single-objective light-sheet; A. Millett-Sikking, K.M. Dean, R. Fiolka, A. Fardad, L. Whitehead and A.G. York; (2019) https://doi.org/10.5281/zenodo.3244420
11. [Diel 2020] Tutorial: avoiding and correcting sample-induced spherical aberration artifacts in 3D fluorescence microscopy; E.E. Diel, J.W. Lichtman and D.S. Richardson; (2020) https://doi.org/10.1038/s41596-020-0360-2
12. [Maioli 2016] Time-lapse 3-D measurements of a glucose biosensor in multicellular spheroids by light sheet fluorescence microscopy in commercial 96-well plates; V. Maioli, G. Chennell, H. Sparks, T. Lana, S. Kumar, D. Carling, A. Sardini and C. Dunsby; (2016) https://doi.org/10.1038/srep37777
13. [Zanacchi 2011] Live-cell 3D super-resolution imaging in thick biological samples; F.C. Zanacchi, Z. Lavagnino, M.P. Donnorso, A.D. Bue, L. Furia, M. Faretta and A. Diaspro; (2011) https://doi.org/10.1038/nmeth.1744
14. [Betzig 2006] Imaging Intracellular Fluorescent Proteins at Nanometer Resolution; E. Betzig, G.H. Patterson, R. Sougrat, O.W. Lindwasser, S. Olenych, J.S. Bonifacino, M.W. Davidson, J. Lippincott-Schartz and H.F. Hess; (2006) https://doi.org/10.1126/science.1127344

GitHub Pages